International Journal of Coal Science & Technology (2022) 9:37
https://doi.org/10.1007/s40789-022-00492-2

RESEARCH

Adsorption mechanism of Cd(II) by calcium-modified lignite-derived humin in aqueous solutions

Ping Wang[1] · Zhanbin Huang[1] · Zhanyong Fu[1] · Peng Zhao[1] · Zeshen Feng[1] · Yao Wang[1] · Fangze Li[1]

Received: 27 July 2021 / Accepted: 16 March 2022

Abstract

Lignite-derived humin (CHM) was extracted from raw coal in Heihe City, China, producing calcium-modified lignite-derived humin (Ca-CHM) by $Ca(OH)_2$. The physical and chemical performances of CHM and Ca-CHM were analyzed with SEM, ^{13}C spectra and XPS techniques. The results show that Ca-CHM exhibited weaker aliphatic, more aromatic polar compared with CHM, which improves the adsorption capacity for Cd(II). XPS analysis indicates that Ca(II) has been loaded onto Ca-CHM successfully after modification. This batch adsorption experiments report the adsorption performance of CHM and Ca-CHM for Cd(II). The adsorption process of CHM and Ca-CHM for Cd(II) conform to pseudo-second-order model, which is chemical adsorption, and the adsorption data presented good fits to the Langmuir model. The maximum adsorption amount (Q_m) of Cd(II) onto CHM and Ca-CHM by the Langmuir model is 15.29 mg/g and 41.84 mg/g, respectively. Based on the results of SEM, ^{13}C spectra, and XPS analysis, we concluded that the main adsorption mechanism of Ca-CHM on Cd(II) was ion exchange of Cd(II) for Ca(II), static-adsorbed and surface complexation. Therefore, Ca(II) can be loaded on the surface of Ca-CHM by chemical modification, improving the adsorption capacity of materials in aqueous solutions.

✉ Zhanbin Huang
zbhuang2003@163.com

[1] School of Chemical and Environmental Engineering, China University of Mining and Technology-Beijing, Beijing 100083, China

Published online: 24 May 2022

Graphical abstract

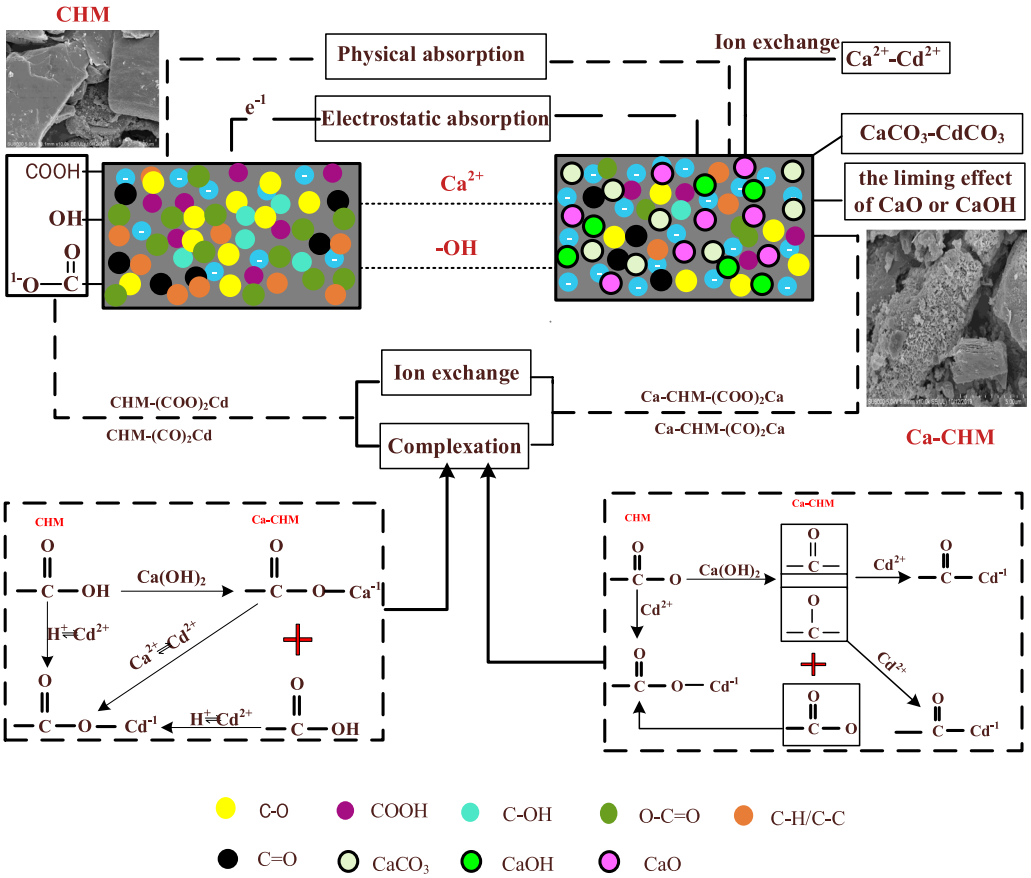

Keywords Lignite-derived humin · Modification · Cd(II) · Adsorption · Mechanism

1 Introduction

Cadmium (Cd) is one of the most widespread and detrimental inorganic pollutants in the natural environment and its compounds can cause many serious diseases of human health (Singh et al. 2012; Sun et al. 2019). Many methods have been conducted to eliminate Cd(II) contamination in wastewater and soil, including physical, chemical, and biological methods. Among them, chemical method is one of the most popular and convenient method for its maneuverability, high efficiency, and low cost. Previous studies have been proven that humin can be a potential adsorbent for adsorbing heavy metals owing to its abundance and cost-effectiveness.

On the basis of the different separation characteristics, humic substances (HS) classified into humic acid (HA), fulvic acid (FA), and humin (HM) (Zomeren and Comans 2007). FA is soluble in both alkaline and acidic solutions, HA is soluble in alkaline solutions, while HM is not soluble insolutions. Much more work has only focused on HA and FA, while on the adsorption of heavy metals by HM (Rosa et al. 2018). Zhang et al. (2018) have reported that humin which was extracted from China's typical black soil was proven to possess the Cr (VI) reduction capability. Although some investigations have been published on humin to adsorb heavy metals (Li et al. 2019; Qiu et al. 2021), these researches were based on the extraction of humin from soil to study the process, mechanism, and effect of heavy metal adsorption. However, no research has been carried out to explore the effect of lignitet-derived humin on heavy metals, mainly due to low adsorption ability of HM. Furthermore, a large of humin left as solid waste residue during the production process of humic acid and fulvic acid from raw coal (Zhang et al. 2021). Owing to the use of alkaline and acid processes, the waste residue was always acid (pH 4–5) or alkaline (pH 9–10), and the adsorption capacity of metal ions is relatively low. The waste residue not only caused the waste of resources, but also posed a potential harm to environment. Therefore, how to improve the adsorption rate of heavy metals by waste residue and transform it into a

resource for heavy metal adsorption is an urgent problem to be solved.

The search for low cost technologies for the removal of heavy metals from the environment has gained interest in recent years. In this sense, the performance of natural or waste materials has been tested and promising results have been published. Relevant researches indicated that some materials through modification could improve adsorption capacity for heavy metals, such as sepiolite, biochar, and fly ash (Deng et al. 2018; Zhang et al. 2019a, b; He et al. 2020). Hydrochars modified by potassium hydroxide improved the Cd removal in water (Sun et al. 2015). Xue et al. (2012) proved that H_2O_2 modified biochar increased the carboxyl groups which showed high Pb(II) removal efficiency. Wan et al. (2021) studied the effects of different cations on the adsorption of cadmium ions by montmorillonite, and found that the action mechanism of cations on cadmium ions was mainly ion exchange reaction, in which Ca^{2+}-montmorillonite > K^+-montmorillonite > Al^{3+}-montmorillonite, indicating that sodium montmorillonite containing calcium element were more conducive to cadmium removal. He et al. (2018) investigated the adsorption of heavy metals by modified peat limestone, and found that the characteristic peaks of Na 1*s*, Ca 2*p* and Al 2*p* disappeared after the adsorption of heavy metals, indicating that Na^+, Ca^{2+} and Al^{3+} adsorbed heavy metal ions through ion exchange. Therefore, for improving the adsorption capacity of the lignite-derived humin, the calcium-modified lignite-derived humin was obtained using $Ca(OH)_2$, so as to confirm the adsorption properties and explore the mechanisms of modified lignite-derived humin for Cd(II). A series of batch adsorption experiments were used to explore the influence factors for adsorption Cd(II), such as pH, initial ions concentrations, and reaction time. The adsorption mechanisms of CHM and Ca-CHM for Cd(II) were explored through SEM, ^{13}C spectra and XPS.

2 Materials and methods

2.1 Materials

Lignite-derived humin was collected from Heihe City, located in Heilongjiang Province, China. The extraction and purification methods of humin were performed in the following steps (Zhang et al. 2013). In order to remove fractions and carbonates, coal sample was mixed with 0.05 M HCl solution. The residue was repeatedly washed by 0.1 M NaOH solution at 25 °C until the colour of supernatants was very shallow. Next, using 0.5% HCl-HF solution to wash the residue three times so as to remove mineral elements, and washing the sample with deionized water until Cl-free ($AgNO_3$ inspection). Finally, we defined it as CHM after the purification of lignite-derived humin. It was dried at 50 °C and stored in an exsiccator for the subsequent experiments.

2.2 Preparation of modified lignite-derived humin

Mixed CHM and $Ca(OH)_2$ according to the mass ratio of 3:2 (w/w) and put the mixture to the 2 L beaker, added 1 L deionized water for 5 days, then washed repeatedly the modified humin until pH = 7. Finally, it was dried to gain calcium-modified lignite-derived humin and defined as Ca-CHM (Jochová et al. 2004).

2.3 Batch sorption experiments

Firstly, the background adsorption solutions of 0.1 M $NaNO_3$ were prepared. Then, $Cd(NO_3)_2{\cdot}4H_2O$ was dissolved in the above solution for preparing the 5000 mg/L of Cd(II), and diluted to the definited concentration in a follow-up experiment.

In batch sorption experiments, put 50 mg sample and mixed with 40 mL Cd(II) solutions into a 100 mL plastic centrifuge tube. The initial solution pH was adjusted to six levels (pH = 2, 3, 4, 5, 6, and 7) with 0.01 M HNO_3 or 0.01 M NaOH. The initial concentrations of Cd(II) were diluted to 10, 20, 50, 80, 100, 150 and 200 mg/L for the sorption thermodynamics. The Cd(II) solution of 100 mg/L was divided into seven reaction time gradients (5, 10, 20, 40, 80, 120, 240, 360 min and 480 min) for the sorption kinetics. The plastic centrifuge tubes were shaken at 25 °C for 24 h to achieve equilibrium. Finally, the mixed solution was separated by 0.45 μm membrane filter and the clear filtrates were analyzed for Cd(II) concentrations by atomic absorption spectrophotometer. The CHM-Cd and Ca-CHM-Cd samples were gained by centrifugation of the mixed solution from the sorption kinetics experiment to analyze the change of functional groups.

The adsorbed amount of Cd(II) is calculated as follows:

$$Q_e = \frac{(C_0 - C_e)V}{m}$$

where Q_e (mg/g) is the amount of Cd(II) adsorption, C_0 (mg/g) and C_e (mg/g) are the concentrations of Cd(II) at the initial and equilibrium concentration, respectively. V (mL) represents the volume of the suspension, and m (mg) represents the mass of the adsorbent.

2.4 Characterization analysis

The micromorphologies, structures and functional groups of CHM and Ca-CHM were analyzed with SEM (Hitachi S-4800), the ^{13}C spectra (Avnce III 400) and XPS techniques (Thermo escalab 250XI). Among them, the samples of CHM

and Ca-CHM were coated with gold during electron microscope scanning.

3 Results and discussion

3.1 Surface characteristics of CHM and Ca-CHM

The surface morphologies of CHM and Ca-CHM were showed in Fig. 1a, b. CHM had a lot of sheet-like structure and possessed a smooth surface (Fig. 1a). The morphology of sample change from smooth surface to little particles and cracks after modification (Fig. 1b), which indicated that the smooth surface of CHM was corroded and dissolved by $Ca(OH)_2$ attacks. Smaller aggregates were formed on the surface of the Ca-CHM after modification, probably associated to the presence of CaOH or CaO precipitates. Ca mineral forms may be present on the humin surface, it may be possible that a fraction of the Cd is bound to this mineral. On the other hand, the presence of Ca on the surface may promote Cd precipitation due to the liming effect of CaO or CaOH.

The ^{13}C spectra were applied to analyze the chemical structure of CHM and Ca-CHM. As we can see from Fig. 1c, the ^{13}C spectra of CHM and Ca-CHM had a similar shape, which was quite similar to the spectra of black soil humin samples that have been reported previously (Zhang et al. 2019a, b). The peaks of CHM and Ca-CHM included alkyl C (0–50 ppm), alkoxy C (50–100 ppm), aromatic C (100–145 ppm), phenol C (145–163 ppm) and carboxylic C (163–200 ppm). The peaks of Ca-CHM at 50–100 ppm and 145–163 ppm increased after modification, which indicated that Ca-CHM had a higher content of alkoxy C and phenolic C. Recent researches have demonstrated that hydroxyl groups and carboxyl groups of material surface played an important role in binding heavy metal ions (Andreas and

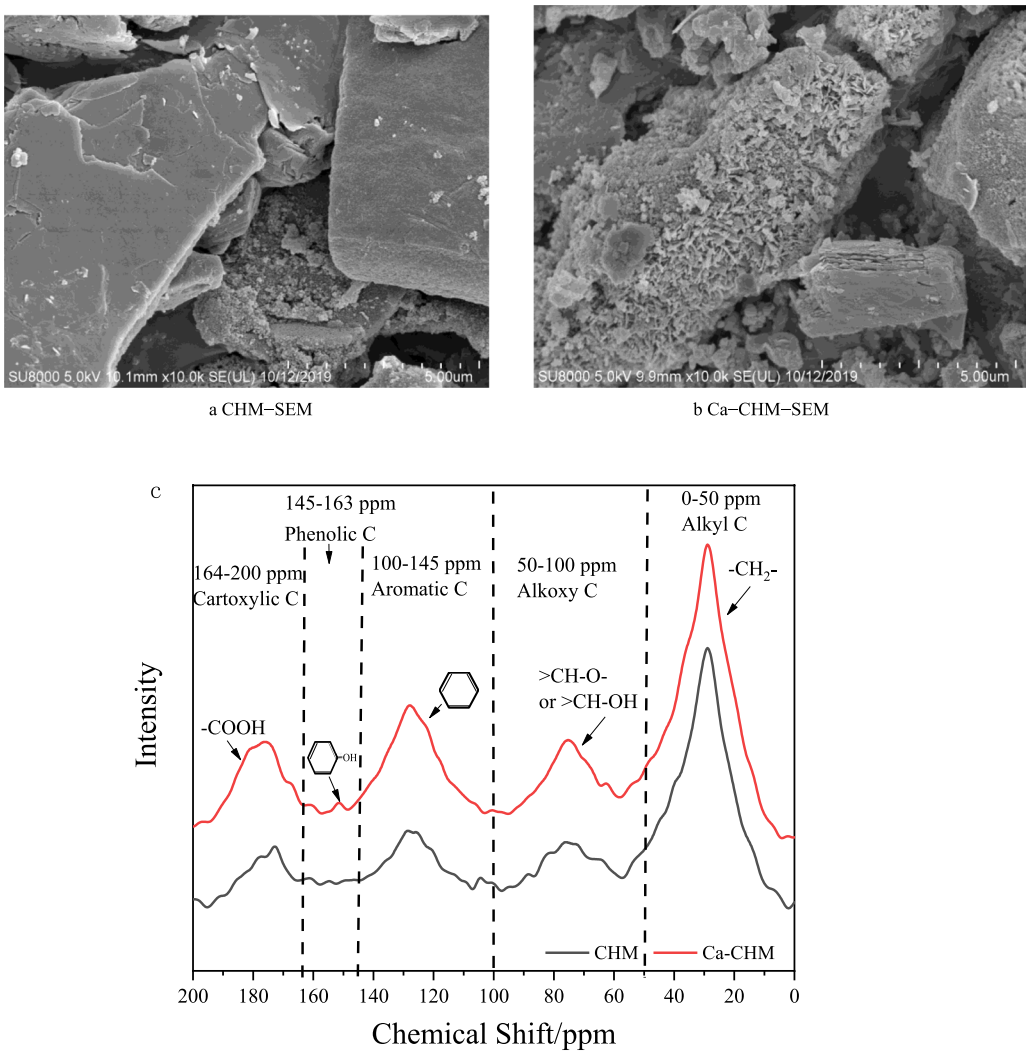

Fig. 1 SEM micrographs of CHM (**a**) and Ca-CHM (**b**). The ^{13}C spectra of CHM and Ca-CHM (**c**)

Zhang 2014; Shi et al. 2018; Yang and Hodson 2018). Therefore, the adsorption capacity of Ca-CHM on Cd(II) may be enhanced due to the increase of alkoxy C and phenolic C.

Table 1 represents the ^{13}C spectra data of CHM and Ca-CHM. Compared with CHM, Ca-CHM contained lager proportions of alkoxy C, aromatic C and carboxylic C, while smaller proportions of $–CH_2–$ and phenolic C. However, CHM was more aliphatic, but the ratios of polar and aromatic polar were lower than that of Ca-CHM. The content of aromatic polar C in Ca-CHM, mainly carboxylic C was much higher than that of CHM, which could be more effective for the Cd(II) adsorption. –COOH is one of the most important functional groups affecting the adsorption of heavy metals. The content of COOH decreased after modification, indicating that Ca^{2+} was loaded on the surface of $(R\text{-}(COO)_2Ca)$. According to the XPS analysis, the characteristic peak of Ca was observed after calcification, which proved that Ca was loaded on the material surface. The content of phenolic C, CH–O– and CH–OH increased, which may be due to the use of $Ca(OH)_2$ modification, and –OH was loaded on the material surface.

3.2 Adsorption studies of Cd(II) on CHM and Ca-CHM

3.2.1 Effect of pH

Many researches have verified that the solution pH can affect the removal efficiency of heavy metal, which also influence the surface charge of materials and the morphology of heavy metals (Chen et al. 2017; Einollahi Peer et al. 2018). As manifested in Fig. 2a, the adsorption amounts of CHM on Cd(II) increased gradually with the increase of solution pH. However, when the pH value was in the range of 2–3, Cd(II) sorption onto Ca-CHM increased sharply, then the effect of changing pH on our research becomes less. Additionally, when pH value was 2, the adsorption amounts of CHM and Ca-CHM on Cd(II) were very low, which was due to the protonated surface of the humin (Naushad et al. 2016). Meanwhile, a large amount of H^+ was bound to the functional groups on the surface of CHM and Ca-CHM, resulting in these groups cannot adsorb Cd(II). The negative functional groups of CHM and Ca-CHM also increased with increasing pH, which was conductive to the combination of negative functional groups and Cd(II). It was worth noting that Cd(II) sorption on Ca-CHM was more steady than that of CHM in the solution pH range from 3 to 7, indicating higher acid neutralizing capacity of Ca-CHM.

3.2.2 Cd(II) adsorption isotherms

For further illustrate the adsorption mechanisms and examine the effect of different Cd(II) concentration onto CHM and Ca-CHM, the Langmuir isotherm model and the Freundlich isotherm model were applied to simulate the adsorption isotherm data (Zheng et al. 2018).

The Langmuir isotherm is described as follows:

$$Q_e = \frac{Q_m K_L C_e}{1 + K_L C_e}$$

The Freundlich isotherm is described as follows:

$$Q_e = K_F C_e^{1/n}$$

where Q_m (mg/g) is the maximum adsorption amount, C_e (mg/L) and Q_e (mg/g) represent the concentration and adsorption amount of Cd(II) at equilibrium, respectively, K_L (L/mg) is the constant referring to the adsorption energy, K_F ((mg/g) $(L/mg)^{1/n}$) and n represent the constant of the binding energy and adsorption intensity, respectively.

The adsorption isotherms of CHM and Ca-CHM on Cd(II) were manifested in Fig. 2b. The adsorption capacity of CHM and Ca-CHM on Cd(II) increased correspondingly with increasing Cd(II) ions concentration. Additionally, the adsorption amount of Ca-CHM on Cd(II) significantly enhanced than that of CHM, which indicated that the modification was successful. Obviously, the excellent adsorption behavior of Ca-CHM on Cd(II) modification signified that Ca-CHM through $Ca(OH)_2$ was beneficial for Cd(II) adsorption.

As showed in Table 2, the fitting parameters in the Langmuir and Freundlich equations were listed. According to the relative parameters, compared with Freundlich ($R^2 < 0.9788$), the Langmuir model had the better fitting

Table 1 Distribution of carbon-containing functional groups of CHM and Ca-CHM by ^{13}C spectra

Sample	Chemical shift (ppm) and carbon assignment (%)					Aliphatic C (%)[a]	Polar[b]	Aromatic polar C (%)[c]
	0–50	50–100	100–145	145–163	163–200			
CHM	61.94	12.63	12.95	3.52	8.95	74.57	25.10	12.47
Ca-CHM	53.63	13.83	18.27	12.78	1.78	67.46	28.39	14.56

[a]Aliphatic C(%): total aliphatic C region (0–100 ppm)

[b]Polar C(%): total polar carbon region (50–100 and 145–200 ppm)

[c]Aromatic polar C(%): total polar carbon region (145–200 ppm)

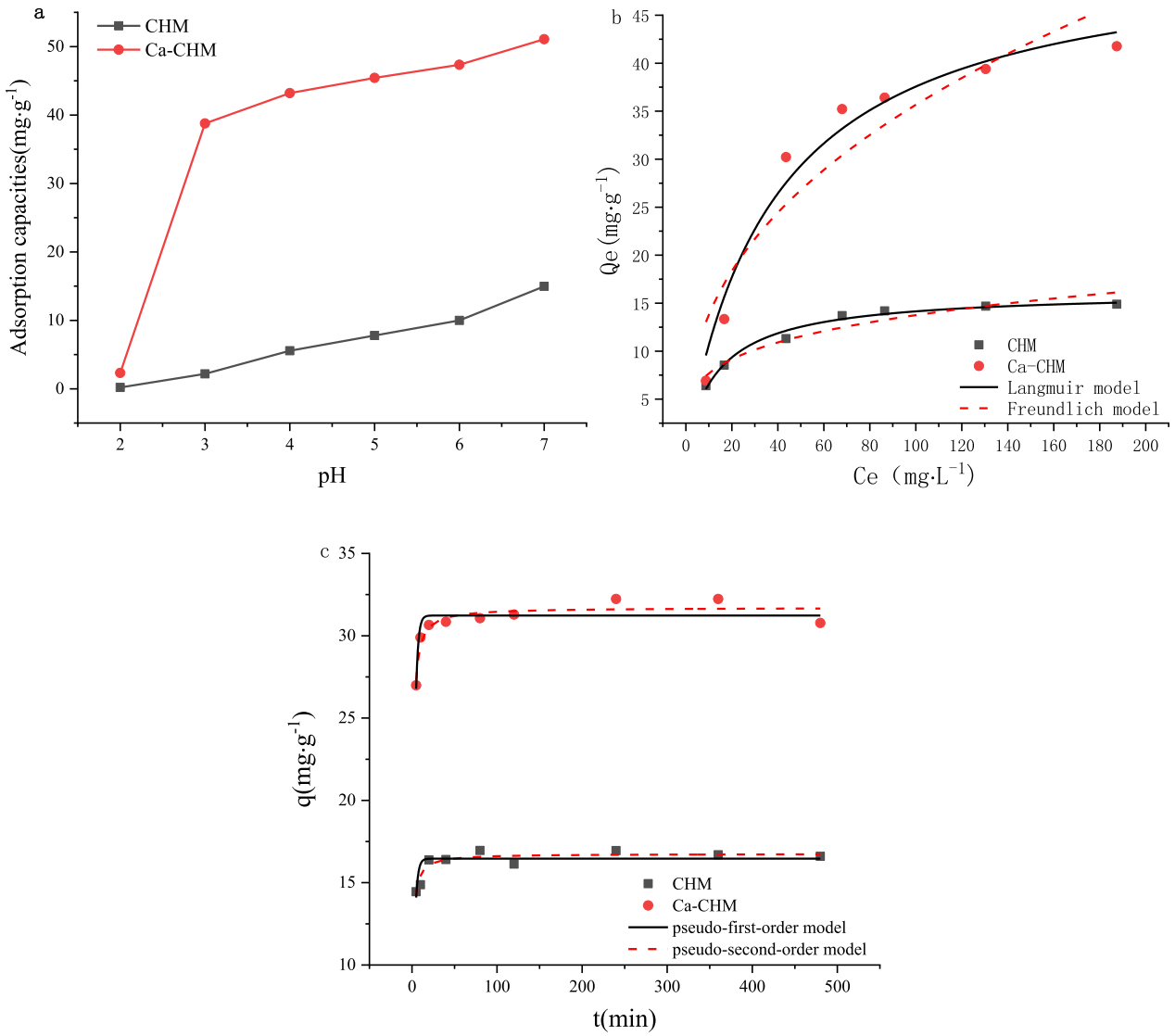

Fig. 2 Effect of Cd(II) adsorption capacities by CHM and Ca-CHM in different pH levels (**a**), Cd(II) concentration (**b**) and reaction time (**c**) Experimental conditions: **a** [(Cd(II) concentration = 100 mg/L, contact time = 24 h, reaction temperature = 25 °C], **b** [pH = 5.5, contact time = 24 h, reaction temperature = 25 °C], **c** [pH = 5.5, Cd(II) concentration = 100 mg/L, reaction temperature = 25 °C]

Table 2 Isotherm parameters of CHM and Ca-CHM to Cd(II)

Thermodynamic model	Parameter	Sample	
		CHM	Ca-CHM
Langmuir	Q_m (mg/g)	15.29	41.84
	K_L (L/mg)	0.1917	0.3621
	R^2	0.9979	0.9978
Freundlich	K_F(L/g)$^{1/n}$	6.2469	14.9865
	n	5.9382	4.1580
	R^2	0.9788	0.9422

curves and the highest R^2 value ($R^2 > 0.9979$), which suggested that the Langmuir model expressed a better adsorption behaviors of Cd(II). In addition, the result revealed that the Cd(II) adsorption onto CHM and Ca-CHM was monolayer and homogeneous(Chen et al. 2019; Almomani et al. 2020). The maximum adsorption amounts of CHM and Ca-CHM for Cd(II) were calculated via the Langmuir fitting model, which was 15.29 and 41.84 mg/g, respectively. The results indicated that Ca-CHM could greatly enhance the Cd(II) adsorption capacity after modification. The constants of the Freundlich model on CHM and Ca-CHM was 5.9382 and 4.1580 ($n > 1$), respectively, indicating that Cd(II) adsorption of CHM and Ca-CHM were

physical adsorption, and the adsorption process was easy to achieve (Zhang et al. 2013).

3.2.3 Cd(II) adsorption kinetics

As presented in Fig. 2c, the adsorption capacity of Cd(II) was rapid remarkably in the initial stage and reached the adsorption equilibrium at 20 min approximately, which signified that the surface of CHM and Ca-CHM had more vacant adsorption sites without adsorbing Cd(II) because of the limited reaction time (Alqadami et al. 2017; Huang et al. 2020). As the reaction time increased, more Cd(II) was adsorbed by anchoring sites onto CHM and Ca-CHM until the adsorption equilibrium. Additionally, the adsorption amount of Cd(II) increased after modification, which indicated that more adsorption sites onto Ca-CHM could adsorb Cd(II).

To explore the Cd(II) adsorption mechanisms onto CHM and Ca-CHM, pseudo-first-order and pseudo-second-order kinetic models were used to calculate adsorption rates and rate-limiting steps (Yang and Hodson 2018; Xiong et al. 2019). The pseudo-first-order and pseudo-second-order could be expressed as the following equations (Wang et al. 2019).

The pseudo-first-order kinetic model is described as follows:

$$Q_t = Q_e(1 - e^{-k_1 t})$$

The pseudo-second-order kinetic model is given as follows:

$$Q_t = \frac{k_2 Q_e^2 t}{1 + k_2 Q_e t}$$

where t (min) is the contact time of adsorbate and adsorbent, k_1 (1/min) and k_2 (g/mg min) are the rate constants of two kinetic models.

Table 3 presents the adsorption kinetics parameters. The correlation coefficients (R^2) of the pseudo-second-order model ($R^2 = 0.9998$, 0.9991) were 0.9998 and 0.9991, respectively, while those of the pseudo-first-order model were 0.6329 and 0.8338, respectively, illustrating that the pseudo-second-order model was applicable to explain the sorption results. Similar researches have been revealed for the adsorption kinetics of heavy metals on the surface of carbon nanotube (Deng et al. 2019), polydopamine microspheres (Sun et al. 2019), which indicated that the adsorption processes were mainly based on chemical adsorption (Zhou et al. 2018; Ahmad et al. 2020).

Table 3 Kinetics parameters of CHM and Ca-CHM to Cd(II)

Kinetic model	Parameter	Sample	
		CHM	Ca-CHM
Pseudo-first-order parameters	Q_e (mg/g)	16.46	31.33
	k_1 (1/min)	0.3880	0.3840
	R^2	0.6329	0.8338
Pseudo-second-order parameters	Q_e (mg/g)	27.47	42.37
	k_2 (g/mg min)	0.2103	0.040
	R^2	0.9998	0.9991

3.3 XPS analysis

Based on the above results, adsorption capacity of Ca-CHM for Cd(II) was much higher than CHM's, which suggested that the surface chemistry took part in the adsorption process of Cd(II). For further clarify the Cd(II) adsorption mechanisms, CHM and Ca-CHM before and after Cd(II) adsorption were analyzed with XPS (Fig. 3).

The survey XPS spectra of CHM and Ca-CHM before and after Cd(II) adsorption were observed in Fig. 3a. The characteristic peaks of Si 2*p*, C 1*s* and O 1*s* were observed onto the surface of CHM, and the peaks of Ca(II) appeared on Ca-CHM after modification, which illustrated that the Ca(II) species were successfully attached to Ca-CHM's surface. The peaks of Cd(II) were clearly observed after the Cd(II) adsorption, which might be due to that the pore and active functional groups were onto the surface of CHM and Ca-CHM through ion exchange, static-adsorbed and surface complexation to Cd(II) adsorption. In addition, the peaks of Cd(II) on Ca-CHM-Cd were higher than those of CHM-Cd, which revealed that the binding capacity of Ca-CHM was more outstanding. The peaks of Ca(II) on Ca-CHM-Cd were smaller than those of Ca-CHM, indicating that Ca(II) took part in the Cd(II) reaction via ion exchanges. Related research showed that Ca(II) is the main mechanism of Cd(II) adsorption from aqueous solution (Chen et al. 2017). Ca-CHM had much higher sorption capacity than that of CHM due to high Ca(II) ion exchange capacity of Ca-CHM. Furthermore, in order to further explore the types of functional groups bound to Cd(II), narrow-spectrum orbitals of C 1*s* and O 1*s* was analyzed for next.

C 1*s* XPS spectra peaks onto CHM and Ca-CHM before and after Cd(II) adsorption were analyzed. As we can see from Fig. 3b, the major C 1*s* peaks at 284.59–284.79 eV, 285.40–286.58 eV, 286.53–286.94 eV and 288.46–289.51 eV were classified as C–C or C–H groups, C–O groups, C=O groups and O–C=O groups, respectively. The distribution of carbon-containing functional groups was briefly summarized in Table 4. Compared with CHM, the values of element (C=O and O–C=O) on CHM-Cd's surface decreased by 22.49%, 5.54% and 1.59%, respectively, indicating that these functional groups made a contribution to Cd(II) adsorption to some extent. The percentage of C–O

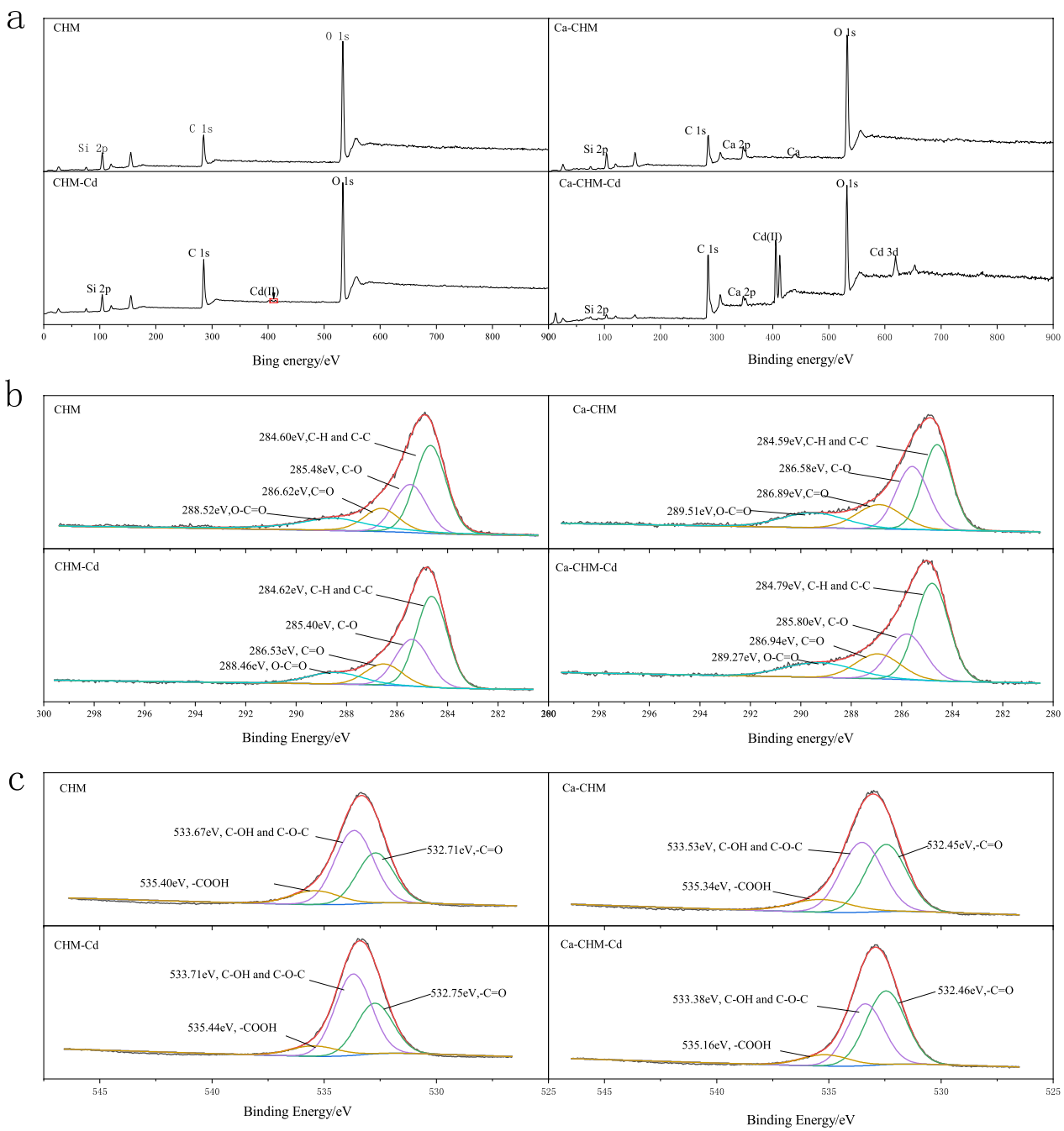

Fig. 3 XPS survey spectra (**a**), C 1*s* (**b**) and O 1*s* (**c**) of CHM and Ca-CHM before and after Cd(II) adsorption

and C=O of CHM increased after modification, while the percentage of O–C=O decreased significantly.

After Cd(II) adsorption, the percentages of C=O and O–C=O of CHM–Cd decreased by 4.86% and 42.28% (Table 4), respectively, indicating that the above functional groups involved in the reaction of Cd(II). After modification, the percentages of C–O and C=O increased, while the percentages of O–C=O decreased significantly. Figure 2a, b shows that Ca $(OH)_2$ has the effect of corrosion and dissolution on the material, which inferred that the decrease of O–C=O may be caused by the fracture of chemical bond during the modification process, resulting in the increase of C=O and C–O. Compared with Ca-CHM, the content of C–O–C, C–OH, and COOH on the surface of Ca-CHM-Cd decreased by 22.49%, 5.54%, and 1.59%, respectively, indicating that these functional groups contributed to the adsorption of Cd(II). Therefore,

Table 4 Distribution of carbon- and oxygen-containing functional groups in CHM and Ca-CHM surface before and after Cd(II) adsorption

Elements	Functional groups	CHM		CHM-Cd		Ca-CHM		Ca-CHM-Cd	
		BE (eV)	RE (%)	BE (eV)	RE (%)	BE (eV)	RE (%)	BE (eV)	RE (%)
C 1*s*	C–C/C–H	284.60	43.47	284.62	48.80	284.59	38.14	284.79	46.09
	C–O	285.48	23.76	285.40	27.06	286.58	30.19	285.80	23.40
	C=O	286.62	13.98	286.53	13.30	286.89	16.62	286.94	15.70
	O–C=O	288.52	18.78	288.46	10.84	289.51	15.05	289.27	14.81
O 1*s*	C=O	532.71	34.50	532.75	34.65	532.45	42.75	532.46	50.94
	C–OH/C–O–C	533.67	52.87	533.71	55.90	533.53	45.42	533.38	39.51
	COOH	535.40	12.63	535.44	9.45	535.34	11.84	535.16	9.54

C–O and C=O groups can be increased by modification, which promotes the adsorption of Cd(II).

It was found that the amount of C–C or C–H groups reduced, while those of the C–O, C=O, and O–C=O groups clearly increased after modification, indicating that Ca-CHM had higher oxygen content.

As manifested in Fig. 3c, the O 1*s* XPS spectra peak onto CHM and Ca-CHM could fit the three curves well: –C=O groups at 532.45–532.71 eV; C–OH or C–O–C groups at 533.38–533.71 eV and –COOH groups at 535.16–535.44 eV. The shifts of –C=O peak, C–OH peak and –COOH peak after Cd(II) adsorption revealed that the electrons were observed to migrate to the oxygen atoms, which signified that ion exchange and surface complexation occurred between the functional group and Cd(II) (Bi et al. 2020). The oxygen contents in different forms onto CHM and Ca-CHM were summarized in Table 4. The results indicated that the quantity of COOH groups and C–O–C groups decreased after modification while that of the C=O groups clearly increased after Cd(II) adsorption. These changes in oxygen contents indicated that they participated in the adsorption reaction of Cd(II) onto CHM and Ca-CHM. The O/C ratio reflects the content of oxygen-containing functional groups such as carboxylic acids in organic materials. Previous studies have proved that the O/C ratios of lignite humic acid and weathered coal were about 0.4 and 0.82, respectively (Gonzalez-Vila et al. 1994; Wang 2018). However, CHM was extracted from the residue of brown fulvic and fulvic acids, which were always abandoned owing to its large molecular weight, few oxygen-containing functional groups and low utilization value. As a kind of macromolecular organic compounds in humus, humin has large molecular weight and is difficult to degrade, accounting for about 50% of the total organic carbon. Furthermore, on the basis of its non-solubility, humin plays a crucial role in the accumulation, transformation, migration and bioavailability of heavy metal pollutants in soil. Bai et al. (2000) had confirmed that the molecular weight of humic acid was related to the complex stability constant of heavy metals. Compared with fulvic acid with smaller molecular weight, humin is more conducive to passivate heavy metals. Additionally, the adsorption of CHM for heavy metals was relatively stable, but the adsorption capacity was low. The adsorption capacity for Cd(II) was greatly improved by modifying the performance. The difficulty of calcium based modification was how to load Ca^{2+} on the surface of CHM, which mainly utilized the corrosiveness of $Ca(OH)_2$ to erode and dissolve CHM, breaking the chemical bond of oxygen-containing functional groups on the surface of Ca-CHM, and Ca^{2+} was successfully loaded on the surface of Ca-CHM, so as to improve the adsorption efficiency of heavy metals and realize the resource utilization of waste residue. However, we didn't infer the important parameters after calcification via the current test, such as the bond energy, bond length among different oxygen-containing groups on the surface of Ca-CHM and Ca^{2+}, as well as the loading amount of Ca^{2+}. Therefore, further research is needed in the future work.

4 Conclusions

In this work, lignite-derived humin (CHM) was extracted from raw coal, then achieving modified lignite-derived humin (Ca-CHM) through $Ca(OH)_2$, which were used for highly efficient adsorption of Cd(II). Compared with CHM, Ca-CHM exhibited a higher content of alkoxyc and carboxylic C, and owned a more preferable adsorption capacity (41.84 mg/g) of Cd(II). Meanwhile, the adsorption process onto CHM and Ca-CHM reached equilibrium within 20 min approximately. The adsorption data of CHM and Ca-CHM were in good agreement with the Langmuir isotherm models and pseudo-second-order kinetic models. Additionally, XPS analysis was applied to explore the adsorption mechanisms. It was attributed to many oxygen-containing functional groups being presented in lignite-derived humin, which might be adsorption Cd(II). The content of oxygen-containing functional groups onto Ca-CHM's surface obviously increased after modification, which could significantly enhance their adsorption capacity. The adsorption mechanism of Cd(II) was cation exchange of Cd(II) for Ca(II),

static-adsorbed and surface complexation. These results suggest that modified lignite-derived humin as a potential absorbent improve the adsorption performance of Cd(II).

Acknowledgements This work was financially supported by the National Key R&D Program of China (No. 2020YFC1806504), Science and Technology Innovation and venture Fund of China Coal Technology and Engineering Group (No. 2020-2-CXY001). We thank the editor and anonymous reviewers for their valuable comments.

Declarations

Conflict of interest No conflict of interest exists in the submission of this manuscript, and the manuscript has been approved by all authors for publication.

References

Ahmad SZN, Wan Salleh WN, Ismail AF, Yusof N, Mohd Yusop MZ, Aziz F (2020) Adsorptive removal of heavy metal ions using graphene-based nanomaterials: toxicity, roles of functional groups and mechanisms. Chemosphere 248:126008

Almomani F, Bhosale R, Khraisheh M, Kumar A, Almomani T (2020) Heavy metal ions removal from industrial wastewater using magnetic nanoparticles (MNP). Appl Surf Sci 506:144924

Alqadami AA, Naushad M, Alothman ZA, Ghfar AA (2017) Novel metal-organic framework (MOF) based composite material for the sequestration of U(VI) and Th(IV) metal ions from aqueous environment. ACS Appl Mater Interfaces 9:36026–36037

Andreas R, Zhang J (2014) Characteristics of adsorption interactions of cadmium(II) onto humin from peat soil in freshwater and seawater media. Bull Environ Contam Toxicol 92:352–357

Bai LY, Chen SB, Hua L, Wen DP (2000) Studies on characteristics of complexation of Cd and Zn with humic acids. J Nucl Agric Sci 14:44–48

Bi J, Huang X, Wang J, Tao Q, Lu H, Luo L, Li G, Hao H (2020) Self-assembly of immobilized titanate films with different layers for heavy metal ions removal from wastewater: synthesis, modeling and mechanism. Chem Eng J 380:122564

Chen G, Shah KJ, Shi L, Chiang P (2017) Removal of Cd(II) and Pb(II) ions from aqueous solutions by synthetic mineral adsorbent: performance and mechanisms. Appl Surf Sci 409:296–305

Chen K, Fan Q, Chen C, Chen Z, Alsaedi A, Hayat T (2019) Insights into the crystal size and morphology of photocatalysts. J Colloid Interface Sci 538:638–647

Deng X, Qi L, Zhang Y (2018) Experimental study on adsorption of hexavalent chromium with microwave-assisted alkali modified fly ash. Water Air Soil Pollut 229:18

Deng S, Liu X, Liao J, Lin H, Liu F (2019) PEI modified multiwalled carbon nanotube as a novel additive in PAN nanofiber membrane for enhanced removal of heavy metal ions. Chem Eng J 375:122086

Einollahi Peer F, Bahramifar N, Younesi H (2018) Removal of Cd(II), Pb(II) and Cu(II) ions from aqueous solution by polyamidoamine dendrimer grafted magnetic graphene oxide nanosheets. J Taiwan Inst Chem Eng 87:225–240

Gonzalez-Vila FJ, Del Rio J, Almendros G, Martin F (1994) Structural relationship between humic fractions from peat and lignites from the Miocene Granada basin. Fuel 73:215–221

He S, Li Y, Weng L, Wang J, He J, Liu Y, Zhang K, Wu Q, Zhang Y, Z (2018) Competitive adsorption of Cd^{2+}, Pb^{2+} and Ni^{2+} onto Fe^{3+}-modified argillaceous limestone: Influence of pH, ionic strength and natural organic matters. Sci Total Environ 637–638:69–78

He X, Jiang J, Hong Z, Pan X, Dong Y, Xu R (2020) Effect of aluminum modification of rice straw-based biochar on arsenate adsorption. J Soils Sediments 20:3073–3082

Huang X, Zhao H, Zhang G, Li J, Yang Y, Ji P (2020) Potential of removing Cd(II) and Pb(II) from contaminated water using a newly modified fly ash. Chemosphere 242:125148

Jochová M, Punčochář M, Horáček J, Štamberg K, Vopálka D (2004) Removal of heavy metals from water by lignite-based sorbents. Fuel 83:1197–1203

Li C, Yan A, Xie X, Zhang J (2019) Adsorption of Cu(II) on soil humin: batch and spectroscopy studies. Environ Earth Sci 78:487

Naushad M, Ahamad T, Sharma G, Al-Muhtaseb AAH, Albadarin AB, Alam MM, Alothman ZA, Alshehri SM, Ghfar AA (2016) Synthesis and characterization of a new starch/SnO_2 nanocomposite for efficient adsorption of toxic Hg^{2+} metal ion. Chem Eng J 300:306–316

Qiu H, Gui H, Fang P, Li G (2021) Groundwater pollution and human health risk based on Monte Carlo simulation in a typical mining area in Northern Anhui Province, China. Int J Coal Sci Technol 8(5):1118–1129. https://doi.org/10.1007/s40789-021-00446-0

Rosa LMT, Botero WG, Santos JCC, Cacuro TA, Waldman WR, Do Carmo JB, de Oliveira LC (2018) Natural organic matter residue as a low cost adsorbent for aluminum. J Environ Manag 215:91–99

Shi W, Lü C, He J, En H, Gao M, Zhao B, Zhou B, Zhou H, Liu H, Zhang Y (2018) Nature differences of humic acids fractions induced by extracted sequence as explanatory factors for binding characteristics of heavy metals. Ecotoxicol Environ Saf 154:59–68

Singh PK, Singh AL, Kumar A, Singh MP (2012) Mixed bacterial consortium as an emerging tool to remove hazardous trace metals from coal. Fuel 102:227–230

Sun K, Tang J, Gong Y, Zhang H (2015) Characterization of potassium hydroxide (KOH) modified hydrochars from different feedstocks for enhanced removal of heavy metals from water. Environ Sci Pollut Res 22:16640–16651

Sun C, Xie Y, Ren X, Song G, Alsaedi A, Hayat T, Chen C (2019) Efficient removal of Cd(II) by core-shell Fe_3O_4@polydopamine microspheres from aqueous solution. J Mol Liq 295:111724

Wan J, Chen WQ, Huang JS, Mou HY, Xue Z, Zhang T (2021) Effect of cations with different valence states on the adsorption of cadmium by montmorillonite. Appl Chem Ind 50:1–13

Wang P (2018) Effects of humic acid on nitrogen transformation, losses and the growth of rape. Shandong Agricultural University, Taian

Wang W, He R, Yang T (2019) Three-dimensional mesoporous calcium carbonate-silica frameworks thermally activated from porous fossil bryophyte: adsorption studies for heavy metal uptake. RSC Adv 8:25754–25766

Xiong C, Wang S, Sun W, Li Y (2019) Selective adsorption of Pb(II) from aqueous solution using nanosilica functionalized with diethanolamine: equilibrium, kinetic and thermodynamic. Microchem J 146:270–278

Xue Y, Gao B, Yao Y, Inyang M, Zhang M, Zimmerman AR, Ro KS (2012) Hydrogen peroxide modification enhances the ability of biochar (hydrochar) produced from hydrothermal carbonization of peanut hull to remove aqueous heavy metals: batch and column tests. Chem Eng J 200–202:673–680

Yang T, Hodson ME (2018) Investigating the potential of synthetic humic-like acid to remove metal ions from contaminated water. Sci Total Environ 635:1036–1046

Zhang J, Wang S, Wang Q, Wang N, Li C, Wang L (2013) First determination of Cu adsorption on soil humin. Environ Chem Lett 11:41–46

Zhang J, Yin H, Wang H, Xu L, Samuel B, Liu F, Chen H (2018) Reduction mechanism of hexavalent chromium by functional groups of undissolved humic acid and humin fractions of typical black soil from Northeast China. Environ Sci Pollut Res 25:16913–16921

Zhang G, Liu L, Shiko E, Cheng Y, Zhang R, Zeng Z, Zhao T, Zhou Y, Chen H, Liu Y, Hu X (2019a) Low-price MnO_2 loaded sepiolite for Cd^{2+} capture. Adsorption 25:1271–1283

Zhang J, Yin H, Wang H, Xu L, Samuel B, Chang J, Liu F, Chen H (2019b) Molecular structure-reactivity correlations of humic acid and humin fractions from a typical black soil for hexavalent chromium reduction. Sci Total Environ 651:2975–2984

Zhang K, Li H, Han J, Jiang B, Gao J (2021) Understanding of mineral change mechanisms in coal mine groundwater reservoir and their influences on effluent water quality: a experimental study. Int J Coal Sci Technol 8(1):154–167. https://doi.org/10.1007/s40789-020-00368-3

Zheng H, Gao Y, Zhu K, Wang Q, Wakeel M, Wahid A, Alharbi NS, Chen C (2018) Investigation of the adsorption mechanisms of Pb(II) and 1-naphthol by β-cyclodextrin modified graphene oxide nanosheets from aqueous solution. J Colloid Interface Sci 530:154–162

Zhou F, Feng X, Yu J, Jiang X (2018) High performance of 3D porous graphene/lignin/sodium alginate composite for adsorption of Cd(II) and Pb(II). Environ Sci Pollut Res 25:15651–15661

Zomeren AV, Comans RNJ (2007) Measurement of humic and fulvic acid concentrations and dissolution properties by a rapid batch procedure. Environ Sci Technol 41:6755–6761